Effect of nanoholes on the vortex core fermion spectrum and heat transport in p-wave superconductors

2013 J. Phys.: Condens. Matter 25 075701

(http://iopscience.iop.org/0953-8984/25/7/075701)

IOP PUBLISHING JOURNAL OF PHYSICS: CONDENSED MATTER

J. Phys.: Condens. Matter **25** (2013) 075701 (6pp) doi:10.1088/0953-8984/25/7/075701

Effect of nanoholes on the vortex core fermion spectrum and heat transport in p-wave superconductors

B Rosenstein[1,2], **I Shapiro**[3] **and B Ya Shapiro**[3]

[1] Department of Electrophysics, National Chiao Tung University, Hsinchu, Taiwan, Republic of China
[2] Applied Physics Department, Ariel University Center of Samaria, Ariel 40700, Israel
[3] Department of Physics, Institute of Superconductivity, Bar-Ilan University, Ramat-Gan 52900, Israel

Received 30 October 2012, in final form 27 December 2012
Published 17 January 2013
Online at stacks.iop.org/JPhysCM/25/075701

Abstract

The spectrum of core excitations of the Abrikosov vortex pinned by a nanohole of the size of the coherence length is considered. While the neutral zero energy Majorana core state remains intact due to its topological origin, the energy of charged excitations is significantly enhanced compared to that in the unpinned vortex. As a consequence of the pinning the minigap separating the Majorana state from the charged levels increases from Δ^2/E_F (E_F is the Fermi energy and Δ is the bulk p-wave superconducting gap) to a significant fraction of Δ. Suppression of the thermodynamic and kinetic effects of the charged excitations allows us to isolate the Majorana state so it can be used for quantum computation. It is proposed that thermal conductivity along the vortex cores is a sensitive method to demonstrate the minigap. Using the Butticker–Landauer–Kopnin formula, we calculate the thermal conductance beyond the linear response as a function of the hole radius.

1. Introduction

Spin-triplet p-wave superfluids, both neutral, such as liquid He^3 (and recently generated by the Feshbach resonance on Li^6 and K^{40}), and charged, such as the superconducting material Sr_2RuO_4 and possibly heavy fermion UPt_3, have given results that are very important to physics [1]. The condensate is described by a generally tensorial complex order parameter Δ exhibiting great variety of the broken symmetry ground states. The broken symmetry and boundary conditions give rise to a continuous configuration of the order parameter as nontrivial topological excitations [2]. Especially interesting is the case of the so-called topological superconductors, characterized by the presence of electron–hole symmetry and the absence of both the time-reversal and spin–rotation symmetry. Realizations of topological p-wave superfluids are chiral superconductors like Sr_2RuO_4, with order parameter of the $p_x \pm ip_y$ symmetry type [3] and the ABM-phase [1] of superfluid He^3 and other fermionic cold atoms [4] and topological superconductor $Cu_xBi_2Se_3$ that produces an equivalent pseudospin system on its surface [5].

The magnetic field in type II superconductors easily creates stable line-like topological defects, Abrikosov vortices [6], see figure 1(a). In the simplest vortex the phase of the order parameter rotates by 2π around the vortex and each vortex carries a unit of magnetic flux Φ_0. Quasiparticles near the vortex core 'feel' the phase wind by creating a set of discrete low-energy Andreev bound states. For the s-wave superconductors when the vortices are unpinned (freely moving) these states have been comprehensively theoretically studied including the excitation spectrum [7], density of states [8], their role in vortex viscosity [6], and the contribution to heat transport [9] and to microwave absorption [10]. The low lying spectrum of quasiparticle and hole excitations is equidistant, $E_l = l\omega$, where angular momentum l takes half integer values. The 'minigap' in the s-wave superfluids is of the order of $\omega = \Delta^2/E_F \ll \Delta$, where Δ is the energy gap and E_F is the Fermi energy.

Free vortices in the p-wave superconductors exhibit a remarkable topological feature in the appearance of the zero energy mode in the vortex core [11]. The spectrum of the low-energy excitations remains equidistant, $E_l = (l-1)\omega$, but now l is an integer [12]. The zero mode represents

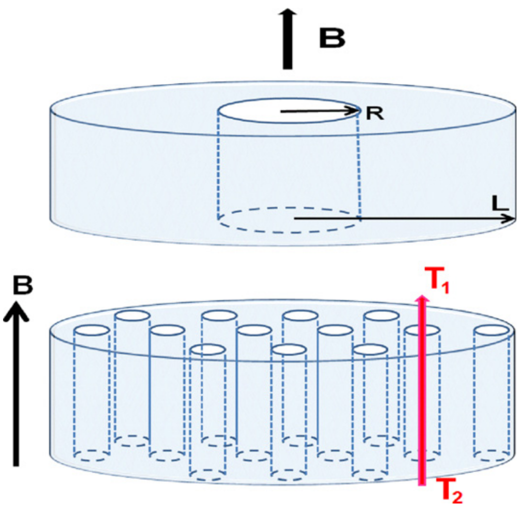

Figure 1. (a) A single vortex in a type II superconductor in magnetic field pinned on an insulator insertion of radius $R \sim \xi$ parallel to the field. The radius of the superconducting disk is $L \gg \xi$. The geometry is used to calculate the spectrum of the chiral p-wave core states. (b) Heat flow through a superconductor in a magnetic field along the vortex cores. The temperature difference between the bottom (T_2) and the top (T_1) contacts leads to energy flow carried by charged core states. Numerous vortices are pinned in inclusions and might be arranged as a lattice.

a condensed matter analog of the Majorana fermion first noticed in elementary particle physics [13]. Its remarkable feature is linked to the fact that its creation operator is identical to its own annihilation, called the Majorana state. Its topological nature ensures robustness against perturbations from deformations of order parameters and nonmagnetic impurities. The states obey non-Abelian statistics with their pairs constituting a qubit. This might offer a promising method for fault-tolerant quantum computation [16]. The main issue is to isolate the states from those above the minigap [14].

The $l = 1$ Majorana mode in the p-wave vortex states has been a popular topic of study over the last few years [12, 17, 15, 18]. While the minigap in the s- and d-wave superconductors was detected by STM [21], it has not been observed in the p-wave. The major reason for this is the *small value of the minigap* ω in the core spectrum (just mK for Sr_2RuO_4). To address this problem a trend was to propose increasingly sophisticated combinations of materials and geometries. For example, one of the proposals [20] to expose the Majorana state is to induce the s-wave superconductivity by the proximity effect on the surface of a topological insulator. The minigaps of the resultant non-Abelian states can be orders of magnitude larger than in a bulk chiral p-wave superconductor.

In this paper we propose to solve the Majorana minigap problem within the original system, a $p_x + ip_y$ bulk superconductor in magnetic field, by pinning the vortices on artificially fabricated dielectric inclusions of the radius comparable to the coherence length ξ of the superconductor [22]. It was shown theoretically [24] that in the s-wave superconductors pinning by an inclusion of radius of just $R = 0.2$–0.5ξ dramatically changes the subgap excitation spectrum; the minigap $\omega \sim \Delta^2/E_F$ becomes of the order of Δ. In the present paper we present the spectrum and wavefunctions of the core excitations in the chiral p-wave superconductor. The charged states for $R = 0.1$–0.4ξ are significantly pushed up towards Δ, so that they therefore interfere less with the Majorana state. To expose the modified charged spectrum, we propose to measure heat transport along the vortex axis, see figure 1(b). The temperature gradient between the top side and the bottom side drives heat along the vortex axis [9]. The exponential temperature dependence of thermal conductivity is very sensitive to the minigap. The temperature when the material undergoes isolator—thermal conductor crossover rises from $\Delta/100$ for unpinned vortices to $\Delta/10$ for inclusion radius $R = 0.4\xi$.

2. Basic equations

We start with the Bogoliubov–de Gennes (BdG) equations for the $p_x + ip_y$ superconductor in the presence of a single pinned vortex. The vector potential $\mathbf{A}$ in polar coordinates, r, φ, has only an azimuthal component $A_\varphi(r)$ and in the London gauge consists of the singular part $A_\varphi^s = h.c./2er$ and the regular part of the vector potential that can be neglected for a type II superconductor [12]. In the operator matrix form for a two component amplitude the BdG equations read

$$\begin{pmatrix} \hat{H}_0 & L \\ L^+ & -\hat{H}_0^* \end{pmatrix} \begin{pmatrix} u \\ v \end{pmatrix} = E \begin{pmatrix} u \\ v \end{pmatrix}, \tag{1}$$

where for anisotropic dispersion

$$\begin{aligned} H_0 &= -\frac{\hbar^2}{2m_\perp}\nabla_\perp^2 - \frac{\hbar^2}{2m_z}\nabla_z^2 - E_F; \\ L &= -\frac{\Delta}{k_F}\left\{ s(r)e^{i\varphi}\left(i\nabla_x - \nabla_y\right) + \frac{1}{2}\left[\left(i\nabla_x - \nabla_y\right) s(r)\, e^{i\varphi}\right]\right\}, \end{aligned} \tag{2}$$

with Δ being the 'bulk gap' of order T_c. The equations, possess electron–hole symmetry. The ansatz

$$\begin{aligned} u &= \frac{1+i}{\sqrt{2}} f(r)\, e^{il\varphi} e^{ik_z z} \\ v &= \frac{1-i}{\sqrt{2}} g(r)\, e^{i(l-2)\varphi} e^{ik_z z} \end{aligned} \tag{3}$$

converts them (for any l there are radial excitation levels denoted by n) into a dimensionless form

$$\begin{aligned} &-\gamma\left(\frac{\partial^2}{\partial r^2} + \frac{1}{r}\frac{\partial}{\partial r} - \frac{l^2}{r^2} + \frac{1}{4\gamma^2}\right) f \\ &\quad - 2\gamma\left[s(r)\left(\tfrac{\partial}{\partial r} - \tfrac{l-2}{r}\right) + \tfrac{1}{2}\left(s'(r) - \tfrac{s(r)}{r}\right)\right] g = \varepsilon_{lk_z} f; \\ &\gamma\left(\frac{\partial^2}{\partial r^2} + \frac{1}{r}\frac{\partial}{\partial r} - \frac{(l-2)^2}{r^2} + \frac{1}{4\gamma^2}\right) g \\ &\quad + 2\gamma\left[s(r)\left(\tfrac{\partial}{\partial r} + \tfrac{l}{r}\right) + \tfrac{1}{2}\left(s'(r) - \tfrac{s(r)}{r}\right)\right] f = \varepsilon_{lk_z n} g, \end{aligned} \tag{4}$$

with dimensionless energy $\varepsilon_{lk_z n} = E_{lk_z n}/\Delta$. Here distances are in units of ξ. We chose the order parameter as a discontinuous function vanishing inside the core $r < R$ and $s = \tanh(r)$ for $r > R$. (The question of justification of using this form, which is often used instead of the fully self-consistent approach, was extensively studied in the literature on both s-wave and non-conventional pairing [8, 12].) In the limit of Bardeen–Cooper–Schrieffer (BCS) theory (applicable to $SrRu_2O_4$) $\xi = \hbar k_\perp / m_\perp \Delta$, where

$$k_\perp^2/2m_\perp = E_F/\hbar^2 - k_z^2/2m_z, \tag{5}$$

and for given k_z there is just one dimensionless parameter

$$\gamma = 1/2k_\perp \xi = m_\perp \Delta / 2\hbar^2 k_\perp^2. \tag{6}$$

The ansatz equation (3) was chosen in such a way that the equations become real. In the presence of a hole of radius R we assume that the order parameter profile is still accurate for $r > R$. In a microscopic theory of the superconductor–insulator interface (see [23]), the order parameter rises abruptly from zero in the dielectric, where amplitudes of normal excitations $f = g = 0$, to a finite value inside the superconductor within an atomic distance a from the interface, namely with a slope $\propto 1/a$. This means that the boundary condition on the amplitudes is consistent with the zero order parameter at the boundary point $r = R - a$ in the self-consistency equation. The sample will be cylindrical with radius L, see figure 1(a).

3. Vortex core spectrum

Qualitatively the spectrum of a single vortex in a hollow disk with internal and external radii R and L consists of two Majorana states, several pairs of Andreev bound subgap states both quasiparticles and holes (related to each other by the electron–hole symmetry) and a continuum of states above a threshold at T_c. The spectrum was calculated numerically by using NAG Fortran Library Routine Document F02EBF. It computes all the eigenvalues, and optionally all the eigenvectors, of a real general matrix, for various values of the inclusion radius $R = 0 \sim 0.9\xi$, external radius $L \sim 10$–20 and the universal parameter $\gamma(k_z) = 1/2k_\perp\xi \sim 10^{-3} - 3 \cdot 10^{-2}$. For sufficiently small l, in addition to the continuum of states above the superconducting gap with $n \geq 1$, there are bound Andreev states that correspond to the lowest $n \equiv 0$. For $l = 1$ and various inclusion radii R there is the Majorana state, for which $f(r) = g(r)$ near the 'internal surface' extending to a distance ξ into the superconductor, see figure 2(a) (see also [18] where the asymptotically exact solution for the Majorana wavefunction is presented for a free vortex) where the radial density

$$\rho(r) = 2\pi r \left(|f(r)|^2 + |g(r)|^2 \right), \tag{7}$$

is given for sufficiently large external radius of the cylinder, $L = 20$ and $\gamma = 0.03$. As was noticed in [17], the function oscillates with period $1/k_\perp\xi$. There is also the second Majorana mode on the 'external' surface for which $f(r) = -g(r)$, given in figure 2(b). The energy of the both states is exponentially small $\varepsilon_{1k_z} \propto e^{-L}$ due to tunneling between them [19]. The surface state wavefunction is almost independent of the inclusion radius for all values of R considered, although it does depend on L. When one considers a small cylinder of the width of several coherence lengths like the one shown in figure 1(a), the two Majorana modes start to overlap. All the other $l = 1$ excitations, $n \geq 1$, are above the threshold and will not be considered and the index is omitted.

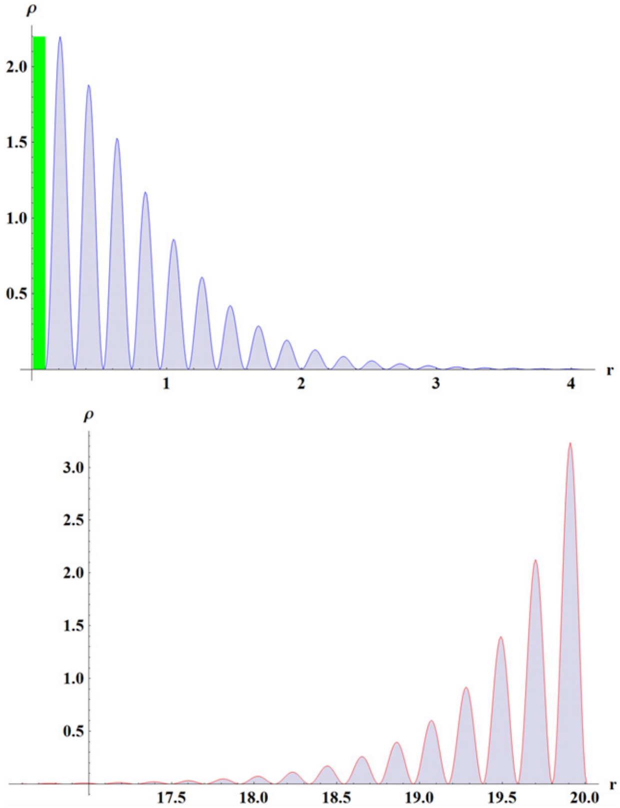

Figure 2. (a) The radial density $\rho(r)$, equation (7), of the Majorana core mode localized on the inclusion (green area) of radius $R = 0.2\xi$ as a function of the distance from the vortex center. The value of the only parameter characterizing the system is $\gamma = 0.03$. The energy of the state is exponentially small as a function of the sample radius L. The wavefunction is pushed out of the center by the inclusion, but otherwise remains intact compared to the unpinned vortex. It extends several coherence lengths inside the superconductor. (b) The radial density $\rho(r)$ as a function of the distance from the vortex center, equation (7), of the Majorana mode localized on the surface of the sample at $r = L = 20\xi$. Due to tunneling to the Majorana core state it also has a negligible energy.

At angular momenta $l \neq 1$ topology does not protect the energy (more precisely its absolute value). The wavefunction of bound states is pushed out of its position near the vortex core when the inclusion is absent. The state that was localized low energy at $R = 0$, becomes delocalized and approaches the threshold at $R = 0.2\xi$ and eventually at $R = 0.4\xi$ merges into the threshold. The energies in units of Δ for a wide range of angular momenta l for $R = 0$ (the blue points), 0.1ξ (green), 0.2ξ (red), 0.4ξ (brown) are given in figure 3. The $R = 0$ line is well approximated for $|l| < 10$ by the semiclassical linear formula [11], while for higher momenta it approaches the threshold along a universal curve that is independent of the inclusion radius. When the hole is present, the dependence on l is no longer monotonic. It first rises to a maximum at $l = -1$ and subsequently has a local minimum with energy about that of the $l = 0$ state. Consequently this becomes a new minigap that becomes of the order of the bulk gap already

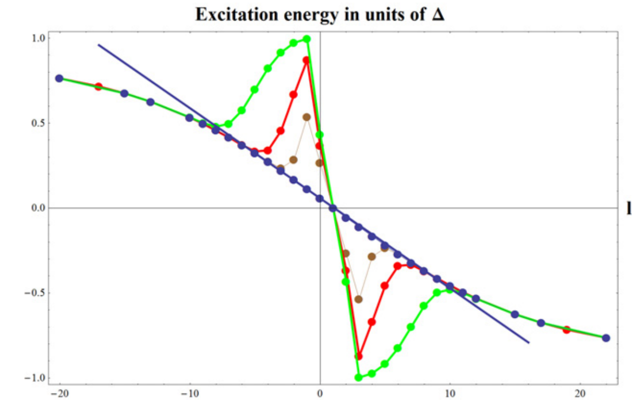

Figure 3. Excitation energy (in units of the bulk gap Δ) of the bound states as a function of angular momentum for several values of the inclusion radius R at $\gamma = 0.03$. For unpinned vortices $R = 0$ (the blue points) the spectrum at small l is described well by the semiclassical formula (see [11]), while for higher momenta it gradually approaches the threshold along a universal curve that is independent of the inclusion radius R. When the inclusion is present the dependence on l is no longer monotonic. It first rises to a maximum at $l = -1$ and subsequently has a local minimum with energy about that of the $l = 0$ state.

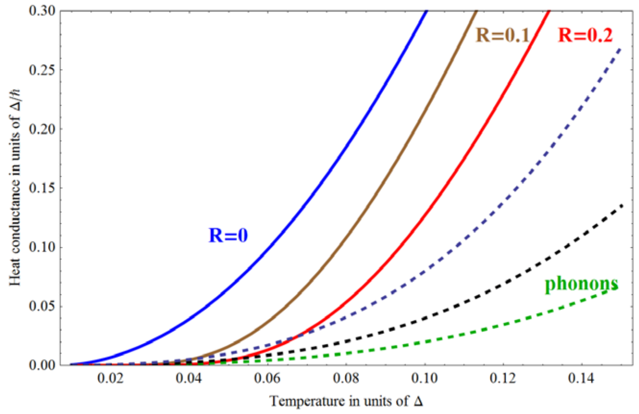

Figure 4. Dimensionless heat conductance $\frac{\hbar}{\Delta}\frac{\mathrm{d}I}{\mathrm{d}T}$ of a single vortex given in equation (12) as a function of inverse temperature in units of Δ^{-1}. The black line is for an unpinned vortex, while the corresponding crossover temperatures from thermal insulator to conductor for pinned vortices on insulating inclusions of radius $R = 0.1\xi$ (brown), $R = 0.2\xi$ (red) are much higher. Dashed lines are the contributions of phonons per vortex for $B = 0.5$ T (green), 0.2 T (black), 0.1 T (blue), length $L_z = 50$ nm, density $n_A = 10^{23}$ cm^{-3}, $\hbar\omega_D = 400$ K.

at relatively small inclusion radius. Beyond this minimum the curve approaches the universal $R = 0$ spectrum, so that wavefunctions are located far from the inclusion. Beyond radius $R = 0.4\xi$ the effect of the minigap enhancement is saturated. Only the value of $\gamma = 0.03$ is shown in figure 3 although dependence on it is very weak for all $\gamma \ll 1$. The enhanced minigap allows us to utilize the Majorana states.

4. Thermal conductivity

Thermal conductivity is an effective tool to demonstrate the minigap due to activated behavior of the electron contribution. To calculate the quasiparticle contribution to thermal conductivity along the vortex cores when the upper side of the vortex line is held at temperature T_1 and the lower side at temperature T_2, see figure 1(b), we use a general ballistic (width of the film L_z smaller than mean free path) Kopnin–Landauer formula [9]. The heat current at temperature lower than the threshold to the continuum of states is carried by the bound core states (except for the Majorana state). For a single vortex it consists of a contribution of quasiparticles and holes

$$I = 2\sum_{l<1} I_l(T_2) - I_l(T_1), \tag{8}$$

$$I_l(T) = \int_0^{k_z^{\max}} \frac{\mathrm{d}k_z}{2\pi\hbar}\left|\frac{\mathrm{d}E_{lk_z}}{\mathrm{d}k_z}\right| \frac{E_{lk_z}}{1+\exp\left(E_{lk_z}/T\right)}, \tag{9}$$

where the energy depends on transferred momentum along the field k_z via γ, see equation (6). The maximal value of k_z is $k_z^{\max} = \sqrt{2m_z E_F}$. Since E_{lk_z} is monotonic the integral can be transformed into

$$I_l(T) = \int_{E_l^0}^{E_F} \frac{\mathrm{d}E}{2\pi\hbar}\frac{E}{1+\exp(E/T)} \approx \frac{T^2}{2\pi\hbar}\Pi\left(\frac{E_{l0}}{T}\right). \tag{10}$$

Since the temperatures are below the threshold, E_F was replaced in the upper limit of the integral by ∞. Here the lower limit of integration is the energy for $k_z = 0$ and

$$\Pi(x) = \pi^2/6 - x^2/2 + x\log\left(1+\mathrm{e}^x\right) + Li_2\left(-\mathrm{e}^x\right), \tag{11}$$

where Li is the polylog function. For small temperature differences the linear response can be used

$$\frac{\hbar}{\Delta}\frac{\mathrm{d}I}{\mathrm{d}T} = \frac{t}{\pi}\sum_{l<1}\left[2\Pi\left(\frac{\varepsilon_{l0}}{t}\right) + \frac{(\varepsilon_{l0}/t)^2}{1+\exp(\varepsilon_{l0}/t)}\right], \tag{12}$$

where $t = T/\Delta$. The values of energies of the core states, presented in figure 3, therefore allow us to calculate the thermal conductivity. In figure 4 the heat conductance of a single vortex line is given as a function of inverse temperature (in units of Δ^{-1}). While for an unpinned vortex (the blue line) the crossover from thermal insulator to conductor is not well defined in the relevant temperature range $\Delta/100 < T < \Delta/4$, for the radius of the inclusion $R = 0.1\xi, 0.2\xi, 0.4\xi$ (brown, red and green respectively) one observes a well defined crossover temperature.

5. Discussion, comparison with the s-wave and conclusions

To summarize, the wavefunctions and the spectrum of the core state well pinned vortices in a chiral p-wave superconductor in a magnetic field was studied, see figure 3. The pinning by a nanohole of the order of coherence ξ is assumed. It is shown that while the neutral Majorana mode is largely intact, all the other Andreev bound states have their energies significantly lifted. The minigap (the energy difference with the Majorana state) is consequently increased from its value for unpinned vortices, Δ^2/E_F, to a fraction of the bulk superconducting gap Δ. In superconductor Sr_2RuO_4 while the minigap for unpinned vortices is just (using [3] $\Delta = 2$ K, $E_F = 10^3$ K) $\omega = 4$ mK, it would become about 0.2 K for a nanohole of radius $R = 0.4\xi = 25$ nm ($\xi = 65$ nm [3]). This would suppress the thermodynamic and transport effects of the charged excitations and allow us to observe the physics of the Majorana state.

It is instructive to compare the results with the corresponding spectrum calculation for the s-wave superconductors given in [24]. The presence of nodes obviously makes the comparison nontrivial. First there is no Majorana mode in the isotropic fully gapped s-wave superconductors. Second there is a difference in the angular momentum of the lowest energy charged excitation. On the basis of hole radius 0.1ξ–0.4ξ calculations indicate (see figure 1 in second reference [24]) that the enhancement for the same hole radius (in units of coherence length) is about the same. However, it occurs at high angular momentum, $l \sim 10$, in the s-wave, while in the p-wave case the $l = 0, 2$ states have the minimal energy. The shape of the spectrum in a p-wave superconductor looks completely different at small l. Note that the p-wave spectrum also has a dip around $l \sim 8$, see figure 3, a bit higher than the minigap at $l = 0$. The physical reason for that is related to the existence of the Majorana state: nodes of the order parameter. While excitations with minimal angular momentum in the s-wave were lifted by the nanohole very close to the threshold (continuum), these states in the p-wave interpolate continuously between the zero energy Majorana state and the threshold. The $l = 0, 2$ states are 'living' near the nodes.

We demonstrated the effect of the enhanced minigap by measuring thermal conductivity along the vortex direction. The activated behavior of the electron contribution per vortex is given in figure 4 and compared to the phonon contribution that dominates at temperatures below $T_m = \Delta/10$. Magnetic field $B \gg H_{c1}$ creates $N = SB/\Phi_0$ vortices, see figure 1(b), over an area S, so that heat conductivity is $\kappa = \frac{L_z B}{\Phi_0}\frac{\mathrm{d}I}{\mathrm{d}T}$, where L_z is the sample width. For $B = 0.5$ T (between H_{c1} and H_{c2} in Sr_2RuO_4), with $R = 25$ nm; $L_z = 70$ nm at $T = 0.2$ K one obtains conductivity $\kappa = 0.05$ W K^{-1} m^{-1}. The phonon contribution in the ballistic regime ($L_z \ll l_{ph}$, where l_{ph} is the phonon mean path) is [25] $\kappa \propto C v_{ph} L_z$ ($v_{ph} \sim \omega_D L_z$ is the phonon velocity, ω_D is the Debye frequency). Taking the phonon heat capacity C in the Debye approximation, one obtains for phonon conductance per vortex

$$\hbar\kappa_{ph}/\Delta = t^3\,(\Delta/\Theta_D)^3\,L_z n_A \Phi_0/B, \tag{13}$$

where Θ_D and n_A are the Debye temperature and the density of the atoms correspondingly. This dependence for various vortex densities presented in figure 4 (dashed lines) demonstrates that for temperatures above the minigap value, the quasiparticle heat conductance clearly dominates. In particular, for parameters $L_z = 50$ nm, $B = 0.5$ T, $a = 0.5$ nm, $T_m = 0.2$ (here a is the inter-atomic distance).

It should be noted that vortices in such an experiment (for the field cooling protocol) will be trapped by the holes rather than by point defects. Those initially not pinned by the holes can be effectively pushed out by a small bias current. Our experimental proposal does not require an ideal hexagonal lattice of identical holes. Periodicity does not play a role and the array may even be random.

Acknowledgment

BYaS and IS acknowledge support from the Israel Scientific Foundation.

References

[1] Leggett A J 1975 *Rev. Mod. Phys.* **47** 331
Legget A J 2006 *Quantum Liquid: Bose Condensation and Cooper Pairing in Condensed-Matter Systems* (Oxford: Oxford University Press)
[2] Salomaa M M and Volovik G E 1987 *Rev. Mod. Phys.* **59** 533
Volovik G E 2003 *Universe in a Helium Droplet* (London: Oxford University Press)
[3] Maeno Y, Hashimoto H, Yoshida K, Nishizaki S, Fujita T, Bednorz J G and Lichtenberg F 1994 *Nature* **372** 532
Mackenzie A P and Maeno Y 2003 *Rev. Mod. Phys.* **75** 657
[4] Sato M, Takahashi Y and Fujimoto S 2009 *Phys. Rev. Lett.* **103** 020401
Bloch I, Dalibard J and Zwerger W 2008 *Rev. Mod. Phys.* **80** 885
[5] Hor Y S, Williams A J, Checkelsky J G, Roushan P, Seo J, Xu Q, Zandbergen H W, Yazdani A, Ong N P and Cava R J 2010 *Phys. Rev. Lett.* **104** 057001
Wray L A 2010 *Nature Phys.* **6** 855
[6] Kopnin N 2001 *Vortices in Type-II Superconductors: Structure and Dynamics* (Oxford: Oxford University Press)
Rosenstein B and Li D P 2010 *Rev. Mod. Phys.* **82** 109
[7] Caroli C, de Gennes P G and Matricon J 1964 *Phys. Lett.* **9** 307
[8] Shore J D, Huang M, Dorsey A T and Sethna J P 1989 *Phys. Rev. Lett.* **62** 3089
Gygi F and Schlüter M 1990 *Phys. Rev.* B **41** 822
Gygi F and Schlüter M 1991 *Phys. Rev.* B **43** 7609
Berthod C 2005 *Phys. Rev.* B **71** 134513
[9] Kopnin N B, Mel'nikov A S and Vinokur V M 2003 *Phys. Rev.* B **68** 054528
[10] Janko B and Shore J D 1992 *Phys. Rev.* B **46** 9270
[11] Kopnin N B and Salomaa M M 1991 *Phys. Rev.* B **44** 9667
Volovik G E 1999 *JETP Lett.* **70** 609
[12] Matsumoto M and Sigrist M 1999 *J. Phys. Soc. Japan* **68** 724
Lu C-K and Yip S-K 2008 *Phys. Rev.* B **78** 132502
Fujimoto S 2008 *Phys. Rev.* B **77** 220501
Sato M and Fujimoto S 2009 *Phys. Rev.* B **79** 094504
[13] Wilczek F 2009 *Nature Phys.* **5** 619
[14] Cheng M, Lutchyn R M and Das Sarma S 2012 *Phys. Rev.* B **85** 165124
[15] Machida K and Nakanishi H 1984 *Phys. Rev.* B **30** 122
Machida K and Fujita M 1984 *Phys. Rev.* B **30** 5284
Stone M and Roy R 2004 *Phys. Rev.* B **69** 184511
[16] Kitaev A 2003 *Ann. Phys.* **303** 2
Ivanov D A 2001 *Phys. Rev. Lett.* **86** 268
Stone M and Chung S-B 2006 *Phys. Rev.* B **73** 014505
Tewari S, Das Sarma S, Nayak C, Zhang C and Zoller P 2007 *Phys. Rev. Lett.* **98** 010506
Nayak C, Simon S H, Stern A, Freedman M and Das Sarma S 2008 *Rev. Mod. Phys.* **80** 1083
[17] Cheng M, Lutchyn R M, Galitski V and Das Sarma S 2009 *Phys. Rev. Lett.* **103** 107001
[18] Gurarie V and Radzihovsky L 2007 *Phys. Rev.* B **75** 212509

[19] Mizushima T and Machida K 2010 *Phys. Rev.* A **82** 023624
[20] Sau J D, Lutchyn R M, Tewari S and Das Sarma S 2010 *Phys. Rev.* B **82** 094522
[21] Hess H F, Robinson R B, Dynes R C, Valles J M and Waszczak J V 1989 *Phys. Rev. Lett.* **62** 214
Shan L *et al* 2011 *Nature Phys.* **7** 325
[22] Nguyen H Q, Hollen S M, Stewart M D, Shainline J, Yin A, Xu J M and Valles J M 2009 *Phys. Rev. Lett.* **103** 157001
Aladyshkin A Yu, Silhanek A V, Gillijns W and Moshchalkov V V 2009 *Supercond. Sci. Technol.* **22** 053001
Misko V R, Bothner D, Kemmler M, Kleiner R, Koelle D, Peeters F M and Nori F 2010 *Phys. Rev.* B **82** 184512
Keay J C, Larson P R, Hobbs K L, Johnson M B, Kirtley J R, Auslaender O M and Moler K A 2009 *Phys. Rev.* B **80** 165421
Sochnikov I, Shaulov A, Yeshurun Y, Logvenov G and Božović I 2010 *Nature Nanotechnol.* **5** 516
[23] DeGennes P G 1966 *Superconductivity of Metalls and Alloys* (New York: Benjamin)
[24] Mel'nikov A S, Samokhvalov A V and Zubarev M N 2009 *Phys. Rev.* B **79** 134529
Rosenstein B, Shapiro I, Deutch E and Shapiro B Ya 2011 *Phys. Rev.* B **84** 134521
[25] Landau L D and Lifshitz E M 1981 *Physical Kinetics* (Oxford: Pergamon Press)